

Soft diffraction dissociation

A Donnachie

Department of Physics, Manchester University*

P V Landshoff

DAMTP, Cambridge University*

Abstract

We refute past suggestions that the data on soft diffraction dissociation demand modifications to conventional Regge theory.

Hard diffractive processes have been an active area of study at HERA and the Tevatron, and will continue to be so at the CERN LHC, but one must be uneasy about all theoretical analyses if we do not even understand soft diffraction. The data^{[1][2]} from the CERN ISR for soft diffraction dissociation,

$$pp \rightarrow pX \quad (1)$$

with the proton emerging with almost no energy loss, have been shown^{[3][4]} to be in good agreement with the triple-Regge description^{[5][6]}. However, the higher-energy data from the CERN SPS collider^{[7][8]} do not show the increase of the cross section with energy expected from simple fits^[6]. This has led certain authors^{[5][9]} to introduce unconventional features into the data analysis, which yield energy dependence in conflict with the standard notions of Regge theory^{[10][6]}. In this paper, we show that this is unnecessary and that conventional Regge theory gives an adequate description of the data.

Let $\xi = 1 - x_F$ be the fractional energy loss of the emerging fast proton (or antiproton) and t the squared momentum transfer to it. According to standard Regge theory, when ξ is small enough and the energy large enough the reaction (1) is generated through the very fast proton “radiating” a pomeron, which hits the other proton and breaks it up. This gives

$$\frac{d^2\sigma}{dt d\xi} = D(t, \xi) \sigma^{\text{pp}}(M^2, t) \quad (2)$$

where M is the invariant mass of the system X in (1),

$$M^2 \sim \xi s \quad (3)$$

This factorisation of the differential cross section into a product of a “pomeron flux” factor $D(t, \xi)$ and a pomeron-proton “cross section” σ^{pp} is ambiguous; different definitions in the literature^{[4][11]} differ by a factor of $\frac{1}{2}\pi$ in the definition of $D(t, \xi)$, with a corresponding difference in the definition of σ^{pp} . Our own definition is^[4]

$$D(t, \xi) = \frac{9\beta_P^2}{4\pi^2} (F_1(t))^2 \xi^{1-2\alpha_P(t)} \quad (4)$$

* email addresses: ad@a35.ph.man.ac.uk, pvl@damtp.cam.ac.uk

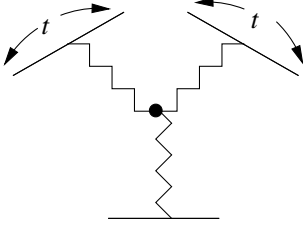


Figure 1: triple-reggeon diagram

where $F_1(t)$ is the proton's Dirac form factor,

$$\begin{aligned} \alpha_{\mathbb{P}}(t) &= 1 + \epsilon_{\mathbb{P}} + \alpha'_{\mathbb{P}} t \\ \epsilon_{\mathbb{P}} &= 0.0808 \quad \alpha'_{\mathbb{P}} = 0.25 \text{ GeV}^{-2} \end{aligned} \quad (5)$$

is the pomeron trajectory and $\beta_{\mathbb{P}}^2 \approx 3.5 \text{ GeV}^{-2}$ is defined such that the pomeron-exchange contribution to the total cross section is^[12]

$$\sigma^{pp}(s) \sim 18 \beta_{\mathbb{P}}^2 (\alpha'_{\mathbb{P}} s)^{\epsilon_{\mathbb{P}}} \cos\left(\frac{1}{2}\pi\epsilon_{\mathbb{P}}\right) = 21.7 s^{0.0808} \quad (6)$$

in mb-GeV units.

Experimentalists commonly integrate $d^2\sigma/dt d\xi = D(t, \xi) \sigma^{\mathbb{P}p}(M^2, t)$ over all t and down to some value M_{MIN} of M , and refer to a total diffractive cross section

$$\sigma^{\text{DIFF}}(s; M_{\text{MIN}}, \xi_{\text{MAX}}) = \int_{M=M_{\text{MIN}}}^{\xi=\xi_{\text{MAX}}} dt d\xi d^2\sigma/dt d\xi \quad (7)$$

The contribution (2) makes $\sigma^{\text{DIFF}}(s; M_{\text{MIN}})$ rise with s almost as fast as $s^{2\epsilon_{\mathbb{P}}}$. As this is faster than the total cross section, it has been claimed^[13] that shadowing effects are important. However, at present energies $\sigma^{\text{DIFF}}(s; M_{\text{MIN}})$ is much less than the total cross section, and so it seems to us likely that shadowing is not yet an issue. This is controversial: for a number of reasons we believe^[6] that shadowing is still unimportant also in forward elastic scattering and in the total cross section, but this view is not universal.

Being a hadronic cross section, $\sigma^{\mathbb{P}p}(M^2, t)$ is expected to be dominated by pomeron exchange when the corresponding centre-of-mass energy M is sufficiently large, and then it becomes proportional to $(M^2)^{\epsilon_{\mathbb{P}}}$, in analogy with the behavior $s^{\epsilon_{\mathbb{P}}}$ of $\sigma^{pp}(s)$ given in (6). When the centre-of-mass energy \sqrt{s} for $\sigma^{pp}(s)$ or M for $\sigma^{\mathbb{P}p}(M^2, t)$ is not large enough, pomeron exchange alone is not sufficient, and nonleading Regge exchanges become important. The dominant such exchange in $\sigma^{pp}(s)$ is f_2 exchange^[6], though ρ , ω and a_2 exchanges are present too. Each of these contributes to $\sigma^{pp}(s)$ a term behaving approximately as $1/\sqrt{s}$. When this is added to the slowly-rising pomeron-exchange term (6), the result is that, as s increases, $\sigma^{pp}(s)$ initially falls with increasing s , and then begins to rise. We expect that f_2 exchange will similarly contribute to $\sigma^{\mathbb{P}p}(M^2, t)$, so that it too falls initially with increasing M , and then begins to rise. Note also the very important point that, for s less than some value s_0 , these exchanges are not sufficient. For most hadron-hadron total cross sections the value of \sqrt{s}_0 is found^[14] to be about 4 to 6 GeV. Similarly, we should expect the simple exchange theory to break down for $\sigma^{\mathbb{P}p}(M^2, t)$ when M is less than some value M_0 . One cannot know what the value of M_0 is; we will be fairly bold and assume a value 3 GeV. This limitation is important when one is interested in the total diffractive cross section $\sigma^{\text{DIFF}}(s; M_{\text{MIN}})$. Usually the value of M_{MIN} that is chosen is less than the likely value of M_0 , in which case the integration over M extends into a region where there is poor theoretical understanding.

According to what we have said, when M is large enough for $\sigma^{\text{IP}}(M^2, t)$ to be approximated by pomeron and other reggeon exchanges, $d^2\sigma/dt d\xi$ in (2) is the sum of triple-reggeon contributions. See figure 1. In this figure, the two upper zigzag lines are the pomeron “radiated” by the very-fast proton. The lower one is the pomeron or reggeon exchanged in $\sigma^{\text{IP}}(M^2, t)$. When ξ is not very small, there are other contributions from a reggeon other than the pomeron being radiated by the very-fast proton. Also, these additional contributions can interfere with the pomeron-radiation term. So we obtain a sum of terms of the type shown in figure 1:

$$\begin{array}{cccccccccc} \mathcal{IP} \mathcal{IP} & \mathcal{IP} \mathcal{IP} & f_2 f_2 & f_2 f_2 & f_2 \mathcal{IP} & \mathcal{IP} f_2 & f_2 \mathcal{IP} & \omega \mathcal{IP} & \dots \\ \mathcal{IP} & f_2 & \mathcal{IP} & f_2 & \mathcal{IP} & \mathcal{IP} & f_2 & \omega & \end{array} \quad (8)$$

The last four terms are examples of interference terms. All the terms but the last contribute equally to $pp \rightarrow pX$ and $\bar{p}p \rightarrow \bar{p}X$ or $p\bar{p} \rightarrow pX$. However the present data turn out not to be sensitive to these terms so we treat $pp \rightarrow pX$ and $\bar{p}p \rightarrow \bar{p}X$ equally. There are also contributions from a_2 and ρ exchange though, as we have said, these couple more weakly to the proton or antiproton. For simplicity we assume that the reggeon exchanges are degenerate. At small t , it is important also to include

$$\begin{array}{cc} \pi\pi & \pi\pi \\ \mathcal{IP} & f_2 \end{array} \quad (9)$$

Altogether, there are a very large number of terms. For each there is a triple-reggeon vertex, the blob in the centre of figure 1, whose dependence on t is completely unknown. With so much freedom, it is surely possible to obtain a good description of the data without having to introduce new and unconventional devices into the fit.

There is a huge amount of data on soft diffraction dissociation. If one plots them one finds that a lot of them are less than good. ISR and SPS collider data have resolution problems for small ξ and so we have restricted our use of these data to $\xi \geq 0.02$. It is a great pity that some of the SPS collider data for $d^2\sigma/dt d\xi$ survives only in integrated form. It is unfortunate that none has been published from the Tevatron, though Goulianos and Montanha^[15] have reconstructed CDF data at $-t = 0.05$ GeV 2 using a particular model. There are some apparently very accurate fixed-target data^[16] though this data set has certain internal peculiarities and at some values of t its normalisation disagrees with that of references [1] and [2], which agree with each other. Figure 2 shows the fixed-target data at two values of s and illustrates that any successful fit must have quite a complicated structure. The differential cross section at fixed ξ decreases with increasing s in this energy range, which is the opposite behaviour from that of the term $\frac{\mathcal{IP}}{\mathcal{IP}}$ in (8). At very small t the differential cross section is very steep and the data cannot be parametrised with a single simple exponential e^{bt} , although this fits satisfactorily at larger t . Simple exponential fits are often used by experimentalists to extrapolate their data beyond the region where they are measured, but this is known to be risky. For example, it is known^[17] that the slope b decreases rapidly as ξ increases.

We have chosen to use collider data from reference [2] at $s = 2880$ GeV 2 . They are relatively smooth, have quite small error bars, and extend over a wide range of t , from $-t = 0.11$ to 0.84 GeV 2 . Note, though, that it may be unsafe to extend the simple Regge-exchange picture to such a large value of t . As we said, to avoid resolution problems we restrict ourselves to $\xi \geq 0.02$ with these data, and at this high energy this corresponds to $M > 7.6$ GeV, comfortably satisfying our condition $M > M_0$ when $M_0 = 3$ GeV. To give leverage in s , we use SPS collider data from reference [7] at $-t = 0.55$ and 0.75 GeV 2 . We use also all the fixed-target data from reference [16]; they are at $s = 262, 309, 366, 565, 741$ GeV 2 and small t , $-t = 0.036, 0.075, 0.131$ and 0.197 GeV 2 . For these low-energy data the constraint $M > M_0$ is important. We use also the reconstructed CDF data^[15] at $-t = 0.05$ GeV 2 .

A simple least- χ^2 fit to these data is not adequate because the error bars on the ISR data are so much larger than on the fixed-target data. So we artificially reduce the error bars on the smallest- t ISR data

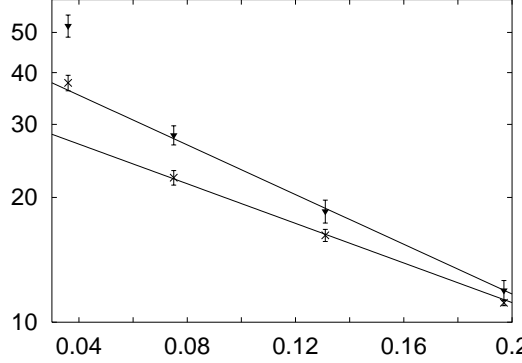


Figure 2: data for $(1/\pi)d^2\sigma/dt d\xi$ in mb GeV $^{-2}$ from reference [16] at $\xi = 0.04$ for $s = 262$ GeV 2 (upper points) and 565 GeV 2 (lower points), plotted against $|t|$. The lines are $46.5 e^{6.9t}$ and $33.5 e^{5.5t}$.

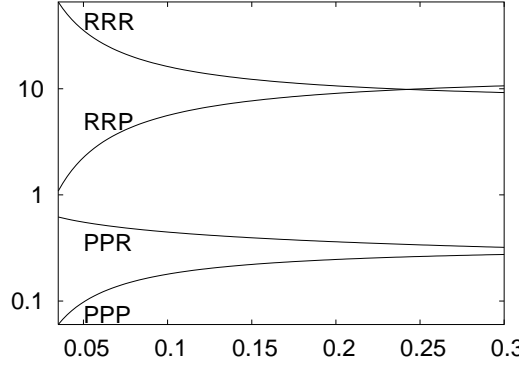


Figure 3: the triple-reggeon vertices plotted against $|t|$

when we make the fit. Also, if we use only the reconstructed CDF data at the one value of t for which it is available, when we integrate the fit over ξ its t dependence is in conflict with what we believe to have been measured by CDF. So we have further reconstructed some CDF data for ourselves, at $-t = 0.01$ and 0.09 GeV 2 with $\sqrt{s} = 1800$ GeV.

Our purpose is to show a reasonable fit to the data within conventional triple-Regge theory, to demonstrate that it is not necessary to introduce any new and unconventional ideas. In order to keep things as simple as possible, we have just used the first seven terms in (8), together with the pion terms (9). The latter contribute only at very small t and are known, essentially without any free parameters:

$$\frac{d^2\sigma^\pi}{dt d\xi} = D^\pi(t, \xi) \sigma^{\pi p}(M^2, t) \quad (10)$$

with

$$D^\pi(t, \xi) = \frac{g_{\pi p}^2}{16\pi^2} \frac{t}{(t - m_\pi^2)^2} (G(t))^2 \xi^{1-2\alpha_\pi(t)} \quad (11)$$

$$\frac{g_{\pi p}^2}{4\pi} = 13.3 \quad \alpha_\pi(t) = \alpha'_\pi (t - m_\pi^2)$$

For the trajectory slope we use $\alpha'_\pi = 0.93$ GeV $^{-2}$. For the form factor $G(t)$, which takes account of the proton wave function, we use the Dirac form factor; this is surely not correct, but it will not matter because $d^2\sigma^\pi/dt d\xi$ is significant only at very small t . For the same reason, we ignore the t

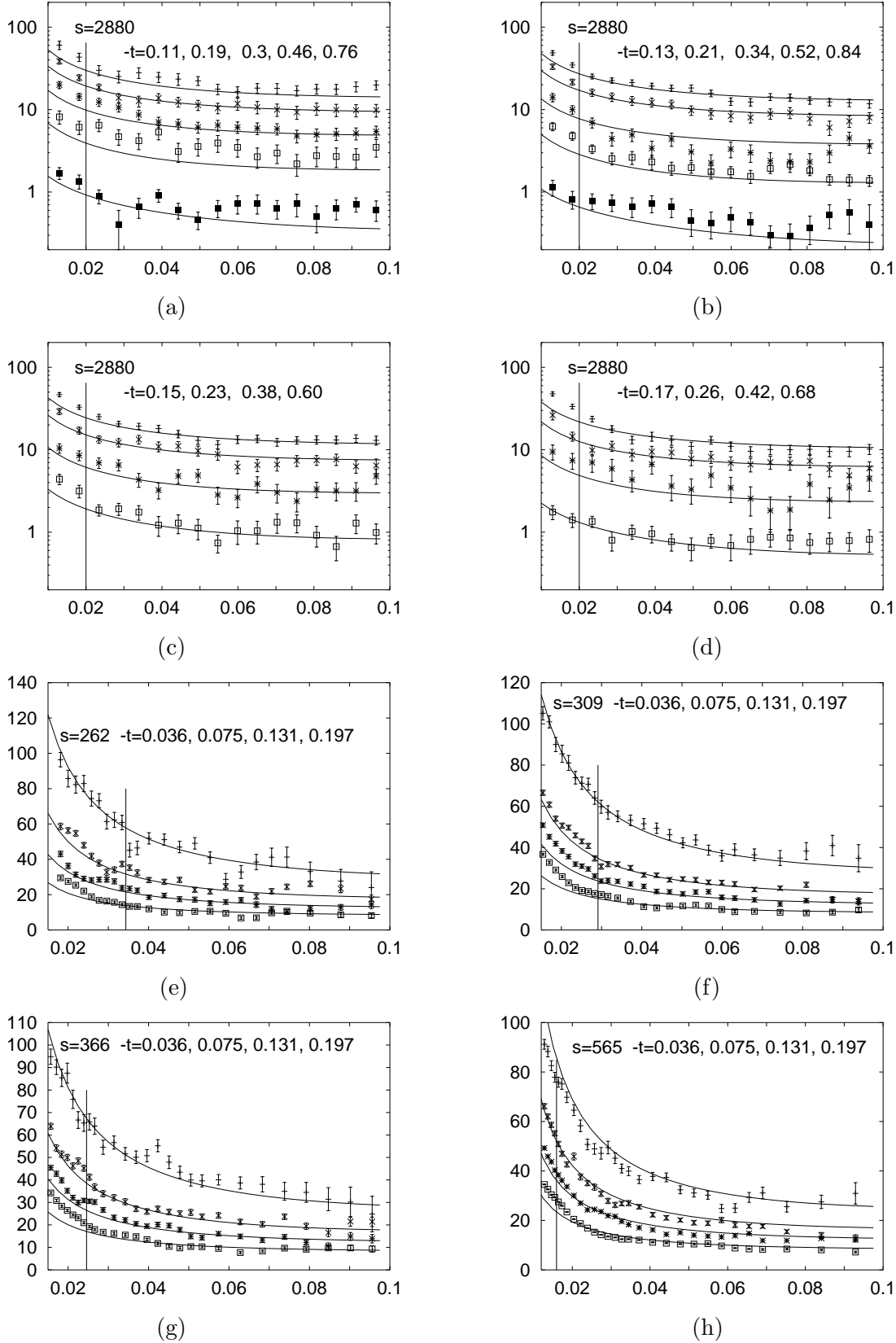


Figure 4: data^[2,16] for $(1/\pi)d^2\sigma/dt d\xi$ in mb GeV $^{-2}$ plotted against ξ at various energies and values of t , compared with the fit. In each case, only data points to the right of the vertical line are used in the fit.

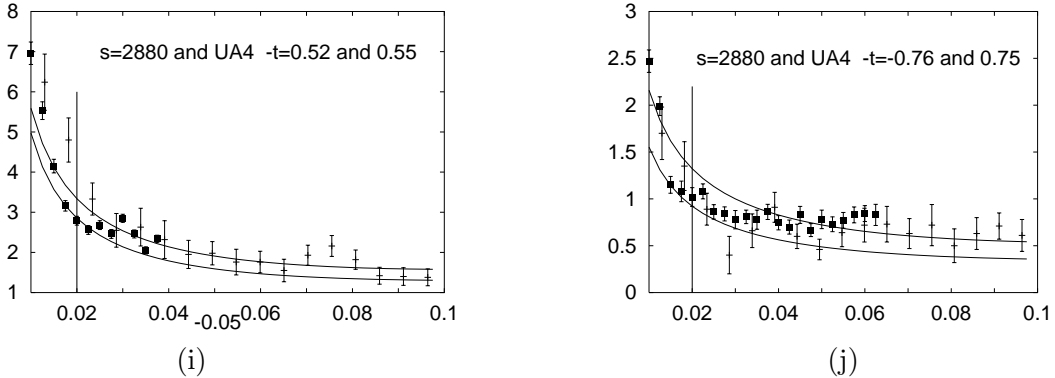


Figure 4 *continued*: open points are from reference [1], black points from UA4[7]. In each case the upper curve is at the higher energy.

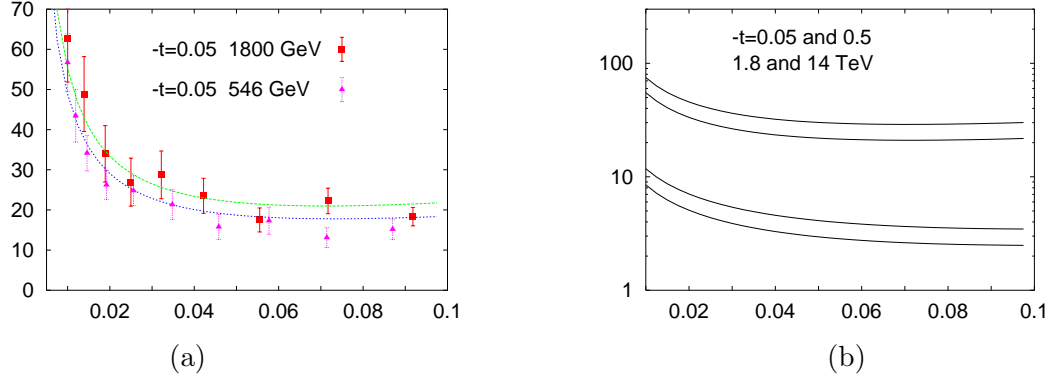


Figure 5: (a) reconstructed CDF data[5] for $(1/\pi)d^2\sigma/dt d\xi$ in mb GeV^{-2} plotted against ξ with our fit; (b) the rise of $(1/\pi)d^2\sigma/dt d\xi$ with \sqrt{s} at $-t = 0.05 \text{ GeV}^2$ (upper pair of curves) and 0.5 GeV^2 . In each case the upper curve is for the higher energy.

dependence of $\sigma^{\pi p}(M^2, t)$ and use its on-shell form^[12]

$$\sigma^{\pi p}(M^2, t) = 13.63 (M^2)^{0.08} + 31.79 (M^2)^{-0.45} \quad (12)$$

We have used a linear f_2 trajectory^[12]

$$\begin{aligned} \alpha_R(t) &= 1 + \epsilon_R + \alpha'_R t \\ \epsilon_R &= -0.45 \quad \alpha'_R = 0.93 \text{ GeV}^{-2} \end{aligned} \quad (13)$$

and an f_2 flux factor

$$D^R(t, \xi) = \frac{9\beta_R^2}{4\pi^2} (F_1(t))^2 \xi^{1-2\alpha_R(t)} \quad (14)$$

with $F_1(t)$ again the proton's Dirac form factor. We also use

$$\begin{aligned} \sigma^{\pi p}(M^2, t) &= V_{\pi\pi\pi}(t) (M^2)^{0.08} + V_{\pi\pi R}(t) (M^2)^{-0.45} \\ \sigma^{Rp}(M^2, t) &= V_{R\pi\pi}(t) (M^2)^{0.08} + V_{RRR}(t) (M^2)^{-0.45} \end{aligned} \quad (15)$$

where the $V_i(t)$ are the triple-reggeon vertices.

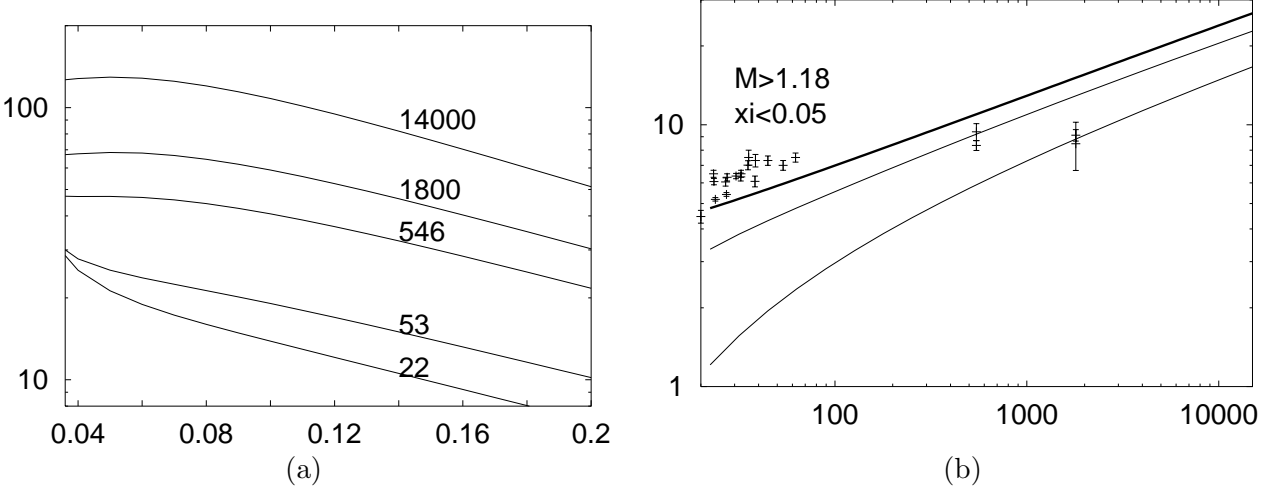


Figure 6: (a) $d\sigma/dt$ in mb GeV $^{-2}$ plotted against $|t|$ for various values of \sqrt{s} ; (b) σ^{DIFF} plotted against \sqrt{s} . Both are for ξ integrated up to 0.05 and down to $M^2 = 1.4$ GeV 2 . In (b) the middle curve is for $-t$ integrated down to 0.036 GeV 2 , the lower curve is the contribution to it from $\frac{I\!P\!P}{I\!P}$ and the upper curve is an estimate for $-t$ integrated down to 0. The data are from the table in reference [15].

It is well tested^[18] in pp elastic scattering that it is the Dirac form factor $F_1(t)$ that takes account of the proton wave function in the coupling of the pomeron to the proton. This is why we have included $F_1(t)$ in the pomeron flux factor $D(t, \xi)$ in (4). The coupling of the reggeon to the proton is less well determined. Nevertheless, we are free to include the same form factor in the reggeon flux factor $D_R(t, \xi)$ in (14), because in the differential cross section it is multiplied by triple-reggeon vertices. There is no knowledge of how these four triple-reggeon vertices depend on t , and the only way we can determine them is to fit their products with the flux factors $D(t, \xi)$ or $D^R(t, \xi)$ to experiment. To this extent, what we choose for the t dependence of the flux factors is just a matter of convention; it is only when one introduces some assumption about the t dependence of the triple-reggeon vertices, or of $\sigma^{I\!P\!P}(M^2, t)$ and $\sigma^{R\!P}(M^2, t)$, that the definitions of the flux factors take on some independent significance.

Previous fits^{[3][4][19]} have included large interference terms, and so we have included such terms maximally. By this we mean

$$\begin{aligned} \frac{I\!P\!R}{I\!P} + \frac{R\!I\!P}{I\!P} &= 2\sqrt{\left(\frac{I\!P\!P}{I\!P} \cdot \frac{R\!R}{I\!P}\right)} \cos\left(\frac{1}{2}\pi(\alpha_{I\!P}(t) - \alpha_R(t))\right) \\ \frac{I\!P\!R}{R} + \frac{R\!I\!P}{R} &= 2\sqrt{\left(\frac{I\!P\!P}{R} \cdot \frac{R\!R}{R}\right)} \cos\left(\frac{1}{2}\pi(\alpha_{I\!P}(t) - \alpha_R(t))\right) \end{aligned} \quad (16)$$

The cosines arise from the Regge signature factors^[6].

We have experimented with various simple forms for the triple-reggeon vertices and have arrived at

$$V_i(t) = A_i \left(\frac{t}{t + \mu_i^2} \right)^{\lambda_i} \quad i = I\!P\!P\!I\!P, I\!P\!P\!R, R\!R\!I\!P, R\!R\!R \quad (17)$$

These are multiplied by the flux factors, which include the couplings $\beta_{I\!P}^2$ or β_R^2 . We have varied the 12 parameters $\beta_i^2 A_i$, μ_i^2 and λ_i to make our fit. It has $\lambda_{R\!R\!R}$ quite large and negative, and $\lambda_{I\!P\!P\!R}$ also negative. One should not conclude from this that the data require that the corresponding vertices

diverge at $t = 0$, because the smallest value of t for which there is data is $-t = 0.036 \text{ GeV}^2$ and it is only for $|t|$ larger than this that our fit has any meaning. As may be seen in figure 3, our vertices all behave sensibly. The reason that V_{RRR} needs to vary fairly rapidly at small t may be seen in figure 2: at least at low energy, the data fall steeply with $|t|$ at very small t and then flatten off. It has been known for a long time^[20] that $V_{\text{PIP}}(t)$ is small at small t .

In figures 4 and 5a we compare our fit with the data we have used, except that we have not shown the $s = 741 \text{ GeV}^2$ data from reference [16] because they are rather ragged. Note that our fit succeeds in reproducing the fact that the data at very small t are higher at low energies than at the Tevatron. Figure 5b shows our expectations for LHC energy; these predictions should be regarded as qualitative because, as we have explained, there is not a sufficient quantity of good lower-energy data to make a definitive fit.

Figure 6a shows $d\sigma/dt$. Although our fit used only data for $M^2 > 9 \text{ GeV}^2$, we have extrapolated it down to 1.4 GeV^2 and integrated over ξ down to this value and up to $\xi = 0.05$. We have multiplied by 2 to account for both $pp \rightarrow pX$ and $pp \rightarrow Xp$ (or $p\bar{p} \rightarrow pX$ and $p\bar{p} \rightarrow X\bar{p}$). We show the plot only down as far as $-t = 0.036 \text{ GeV}^2$, for the reasons we have explained. We have explained also that it is risky to extrapolate the simple fit to values of M below $M_0 = 3 \text{ GeV}$.

Figure 6b shows the integral of $d\sigma/dt$. The middle curve integrates it down to $-t = 0.036 \text{ GeV}^2$ and the lower curve shows how much comes from the term $\frac{\text{PIP}}{P}$. We have extrapolated the curves in figure 6a down to $t = 0$ to get a rough estimate of how much we should add to the middle curve to make it extend to $t = 0$. This extrapolation is highly uncertain. If we assume that between $t = 0$ and $-t = 0.054 \text{ GeV}^2$ $d\sigma/dt$ may be well approximated by a single exponential e^{bt} , so that

$$\sigma(t_{\text{MIN}} = 0) = (\sigma(t_{\text{MIN}} = 0.036))^3 / (\sigma(t_{\text{MIN}} = 0.054))^2 \quad (18)$$

this results in the upper curve. If instead we had used the parametrisation (17) with our large negative λ_{RRR} it would have led to a divergent cross section.

The upper curve in figure 6b fits well to

$$\sigma^{\text{DIFF}}(s; M_{\text{MIN}}^2 = 1.4 \text{ GeV}^2) = 1.9 s^{0.1425} \quad (19)$$

in mb-GeV units. The data are from reference [15]. We must emphasise that experiments all have limited acceptance in t and ξ , so that the values they quote for $\sigma^{\text{DIFF}}(s; M_{\text{MIN}})$ are more than a little model-dependent. As we have just explained, our fit to the available data, which are for $-t \geq 0.036 \text{ GeV}^2$, can give very different total “diffractive” cross sections when it is extrapolated to $t = 0$ in different ways. Because we do fit the available differential-cross-section data, the total diffractive cross section represented by the upper curve in figure 6b is just as believable as the claimed data points; there is no trustworthy extraction of the total diffractive cross section. This in turn leads to uncertainty in the results for σ^{TOTAL} when it is extracted from collider experiments by the so-called luminosity-independent method^[21].

Our fit (6) to the total cross section predicts $\sigma^{\text{TOTAL}} = 101.5 \text{ mb}$ at $\sqrt{s} = 14 \text{ TeV}$, while (19) gives $\sigma^{\text{DIFF}} = 29 \text{ mb}$, so there is no need to introduce significant shadowing up to this energy.

As is seen in figure 6b, even at Tevatron energy the term $\frac{\text{PIP}}{P}$ contributes less than 70% of the total “diffractive” cross section. At very large energies this fraction rises to nearly 80%. Accurate measurement of $d^2\sigma/dtd\xi$ at RHIC would be of great value in clarifying further the details of the diffractive dissociation mechanism.

This research was supported in part by PPARC

References

- 1 M G Albrow et al, Nuclear Phys. B108 (1976) 1
- 2 J C M Armitage et al, Nuclear Physics B194 (1982) 365
- 3 D P Roy and R G Roberts, Nuclear Physics B77 (1974) 240
- 4 A Donnachie and P V Landshoff, Nuclear Physics B244 (1984) 322
- 5 K Goulianos, Physics Letters B358 (1995) 379
- 6 A Donnachie, H G Dosch, P V Landshoff and O Nachtmann, *Pomeron physics and QCD*, Cambridge University Press (2002). See www.damtp.cam.ac.uk/user/pvl/QCD
- 7 UA4 collaboration, M Bozzo et al, Physics Letters B136 (1984) 217
- 8 UA8 collaboration, A Brandt et al, Nuclear Physics B514 (1998) 3
- 9 S Erhan and P E Schlein, Physics Letters B481 (2000) 177
- 10 P D B Collins, *Introduction to Regge Theory and High Energy Physics*, Cambridge University Press (1977)
- 11 E L Berger, J C Collins, D Soper and G Sterman, Nuclear Physics B288 (1987) 704
- 12 A Donnachie and P V Landshoff, Physics Letters B296 (1992) 227
- 13 E Gotsman, E M Levin and U Maor, Physical Review D49 (1994) 4321
- 14 J R Cudell et al, Physical Review D61 (2000) 034019; *erratum* D63 (2001) 059901
- 15 K Goulianos and J Montanha, Physical Review D59 (1999) 114017
- 16 R D Schamberger et al, Physical Review D17 (1978) 1268
- 17 E710 collaboration: N A Amos et al, Physics Letters B186 (1987) 227
- 18 A Donnachie and P V Landshoff, Nuclear Physics B267 (1986) 690
- 19 H1 collaboration, C Adloff et al, Zeitschrift für Physik C74 (1997) 221
- 20 A B Kaidalov, Physics Reports 50 (1979) 157
- 21 CDF collaboration, F Abe et al, Physical Review D50 (1994) 5550

